Humans exploit passive anterior-posterior motion to improve either walking efficiency or walking balance based on environmental risk

Ashwini Kulkarni, Chuyi Cui, Shirley Rietdyk, Satyajit Ambike

Department of Health and Kinesiology, Purdue University, West Lafayette, IN

Keywords: proactive adaptation; adaptive gait; uncontrolled manifold; obstacle crossing

Running title: Synergistic control of MOS in human locomotion

Address for correspondence:

Satyajit Ambike

Department of Health and Kinesiology,

800 West Stadium Ave,

Purdue University,

West Lafayette, IN 47907

USA

Tel: (765) 496-0567

E-mail: sambike@purdue.edu

SUMMARY STATEMENT

Humans maintain specific levels of instability in their gait depending on environmental conditions.

Abstract

In human gait, the body's mechanical energy at the end of one step is reused to achieve forward progression during the subsequent step, thereby reducing the required muscle work. These passive body dynamics, while improving walking efficiency, also indicate unstable gait; the mechanics driving the body forward will be less able to withstand an external perturbation, hence increasing fall risk**.** Here we test the novel hypothesis that passive anterior-posterior (AP) stability is manipulated via active selection of step length to either achieve energy-efficient gait or to improve stability when balance is threatened. We computed the AP margin of stability (MOS_{AP}), which quantifies the passive dynamic stability of gait, for six consecutive steps when healthy young adults (N=20) walked on a clear and on an obstructed walkway. MOS_{AP} values indicated unstable passive dynamics for all steps except while crossing the obstacle with the leading limb (i.e., for the step with the greatest threat to balance). MOS_{AP} increased, indicating more stable dynamics, while approaching and crossing the obstacle with the leading limb, and then declined for later steps. Thus, humans employ a *proactive strategy of manipulating passive dynamics* to meet the demands of the locomotor task. Furthermore, the step length and the center-of-mass motion co-varied to maintain MOS_{AP} for all steps in both tasks at the specific MOS_{AP} value for each step. That is, humans actively regulate step length to maintain specific levels of instability/stability for each step during unobstructed and obstructed gait.

1. Introduction

On a clear, straight path, humans reduce the energy required for walking by selecting appropriate step length (Kuo et al., 2005, Kuo and Donelan, 2010). The selected step length ensures that the kinetic energy at the end of a step is sufficient to passively rotate the body over the new stance foot, thereby achieving forward progression at low energetic cost. In other words, humans exploit the *passive dynamics* of the body to improve energy efficiency (Kuo et al., 2005, Bosse et al., 2012). This energy saving mechanism relies on instability in the gait cycle. There is indeed evidence for instability, reflected in negative values for the margin of stability in the anterior-posterior direction (MOS_{AP}; abbreviations in Table 1) (Ohtsu et al., 2020, Ohtsu et al., 2019, Bruijn et al., 2013). The instability, while improving efficiency, also indicates that the passive dynamics will be less able to resist external perturbations, thereby increasing fall risk (Ohtsu et al., 2020, Bosse et al., 2012). Therefore, exploiting passive dynamics to improve efficiency also increases the threat to balance.

Given this zero-sum situation, humans likely modulate the instability in the passive dynamics to either enhance forward progression or prioritize balance, as the context demands. The threat to balance will be low during unobstructed, straight-line walking, and therefore, unstable passive dynamics will be used to improve efficiency. In contrast, when a locomotor task involves a higher risk of a forward loss of balance, e.g., when risk of tripping is higher, the instability in the forward direction will be reduced (Hak et al., 2013). Anterior passive instability is indeed lower while crossing an obstacle compared to unobstructed gait (Raffegeau et al., 2022, Hak et al., 2019). Since the step length determines the instability (MOS_{AP} is a function of step length and the body's motion), we argue that humans actively select step length to maintain MOS_{AP} in a given locomotor context.

Furthermore, stability changes in motor behaviors cannot occur instantaneously, but must evolve over a characteristic time determined in part by the inertia of the body (Tillman and Ambike, 2020). Therefore, we argue that a shift along the efficiency-stability spectrum will occur over multiple steps – at least for locomotor tasks that afford the time and space for such a shift to occur. For example, while crossing a visible, stationary obstacle, gait stability is altered not only when the feet cross the obstacle (i.e., crossing steps). Rather, changes in stability will

be evident in the steps leading up to the obstacle (i.e., approach steps) to facilitate the transition from unobstructed to obstructed gait. In the approach steps, visual information about the hazard is being gathered (Diaz et al., 2018, Patla and Vickers, 1997) and spatio-temporal gait characteristics (gait speed and foot placement variability) are modified (Muir et al., 2019). However, proactive stability adaptations in the anterior-posterior (AP) direction during approach have not been examined, and it is likely that these stability adaptations are a critical component of maintaining forward progression through challenging environments.

Therefore, our primary goal was to establish that humans control MOS_{AP} during unobstructed as well as obstructed walking. We propose and test the novel hypothesis that the central nervous system responds to changes in the body's motion with a corresponding correction in step length so that the MOS_{AP} itself is invariant at each heel contact. MOS_{AP} will be maintained at different values during unobstructed vs. obstructed walking. Our second goal was to quantify any proactive adaptations in MOS_{AP} while approaching an obstacle. We computed the MOS_{AP} at consecutive heel contacts during unobstructed walking and during an obstacle-crossing task. MOS_{AP} at heel contact is the distance from the anterior boundary of the base of support (the leading heel) to the extrapolated center of mass, or XcoM, which reflects the center of mass (CoM) state (Hof et al., 2005, Hof, 2008). To address our first goal, we employed the uncontrolled manifold (UCM) method (Scholz and Schoner, 1999). For each heel contact, we parsed the across-trial variance in the step length and the XcoM into two components: one that maintained MOS_{AP} (called V_{UCM}) and another that changed MOS_{AP} (called V_{ORT}). We used the normalized excess of V_{UCM} over V_{ORT} as a synergy index. A positive synergy index indicates that MOS_{AP} was actively controlled, i.e., stabilized at the specific across-trial mean MOS_{AP} for that step. A higher value indicates a stronger synergy or higher stability of MOS_{AP}. We emphasize that stability of MOS_{AP} is different from the stability of gait. MOS_{AP} is the measure of gait stability. In contrast, the synergy index indicates the efficacy of control at stabilizing or maintaining MOS_{AP} at a specific value for a given step. To address our second goal, i.e., to identify any proactive changes in gait stability, we compared the MOS_{AP} values for the steps leading up to, while crossing and then resuming unobstructed gait after crossing an obstacle.

We hypothesized that the synergy index will be greater than zero, indicating that the step length and the XcoM co-vary to stabilize MOS_{AP} for all steps in both tasks (H1). In particular, we expect a positive synergy index for both positive and negative MOS_{AP} values (for various steps). Next, we hypothesized a task by step interaction for the synergy index (H2). The synergy index will not be different across tasks (unobstructed and obstructed) for the steps at the start and end of the walkway, but the synergy index will be lower while crossing an obstacle placed in the middle of the walkway. The lower synergy index will reflect the greater motor demands associated with the crossing steps; larger muscle activations required for stepping over the obstacle (Haefeli et al., 2011) will be associated with greater noise (Harris and Wolpert, 1998), which will make stabilization more difficult. Finally, we hypothesized a task by step interaction for MOS_{AP} (H3). The MOS_{AP} will not be different across tasks for the steps at the start and end of the walkway, but the MOS_{AP} will be higher for the approach steps 1-2 steps before the obstacle and for the crossing steps. These changes are consistent with prioritization of safety over energy optimality (Chou et al., 1997, Hak et al., 2019, Bosse et al., 2012).

Table 1. Abbreviations.

Anterior-posterior	AP
Medial-lateral	ML
Foot placements	fp
Center of mass	CoM
Center of mass velocity	V_{CoM}
Leg length	l
Acceleration due to gravity	g
Base of support	BOS
Extrapolated center of mass	XcoM
Margin of stability in anterior-posterior direction	MOS_{AP}
Uncontrolled manifold	UCM
Orthogonal manifold	ORT

Synergy index	ΔV
Synergy index z transformed	ΔV_Z
Variance along the uncontrolled manifold	V_{UCM}
Variance along the orthogonal manifold	V_{ORT}

2. Materials and Methods

2.1 Participants

Twenty-six healthy young adults participated in the study. We excluded six participants due to poor kinematic tracking. Data from 20 participants (14 females, 22.3 ± 3.7 years, 1.7 ± 0.1 m, 66.9 ± 14.6 kg) were used for analysis. All participants walked without aid, had no orthopedic, neuromuscular, or dementia disorders, and were independent in daily activities. Vision was normal or corrected-to-normal. The study was approved by the University's Institutional Review Board, and all participants provided written informed consent.

2.2 Equipment and Procedures

Participants walked at their self-selected speed on a 6.0 m walkway and stepped over an obstacle when present (Fig. 1A). The obstacle was 100 cm wide × 0.4 cm deep. The height of the obstacle was scaled to 25% of the participant's leg length. The obstacle was made of black Masonite and designed to tip if contacted. The starting position was determined for each participant such that they took five steps before reaching the obstacle, crossed the obstacle with the right leg first and stopped three to four steps later (Fig. 1A).

Participants performed 20 trials each of walking with an obstacle (obstacle-crossing task) and walking without an obstacle (no obstacle task). We collected kinematic data at 100 Hz with a motion capture system (Vicon Vero, Oxford, UK) with marker clusters placed bilaterally on the lower back, thigh, shank, and foot. We digitized the joint centers and posterior aspect of the heels to identify their locations relative to the marker clusters. We also digitized the top edge of the obstacle to identify its position.

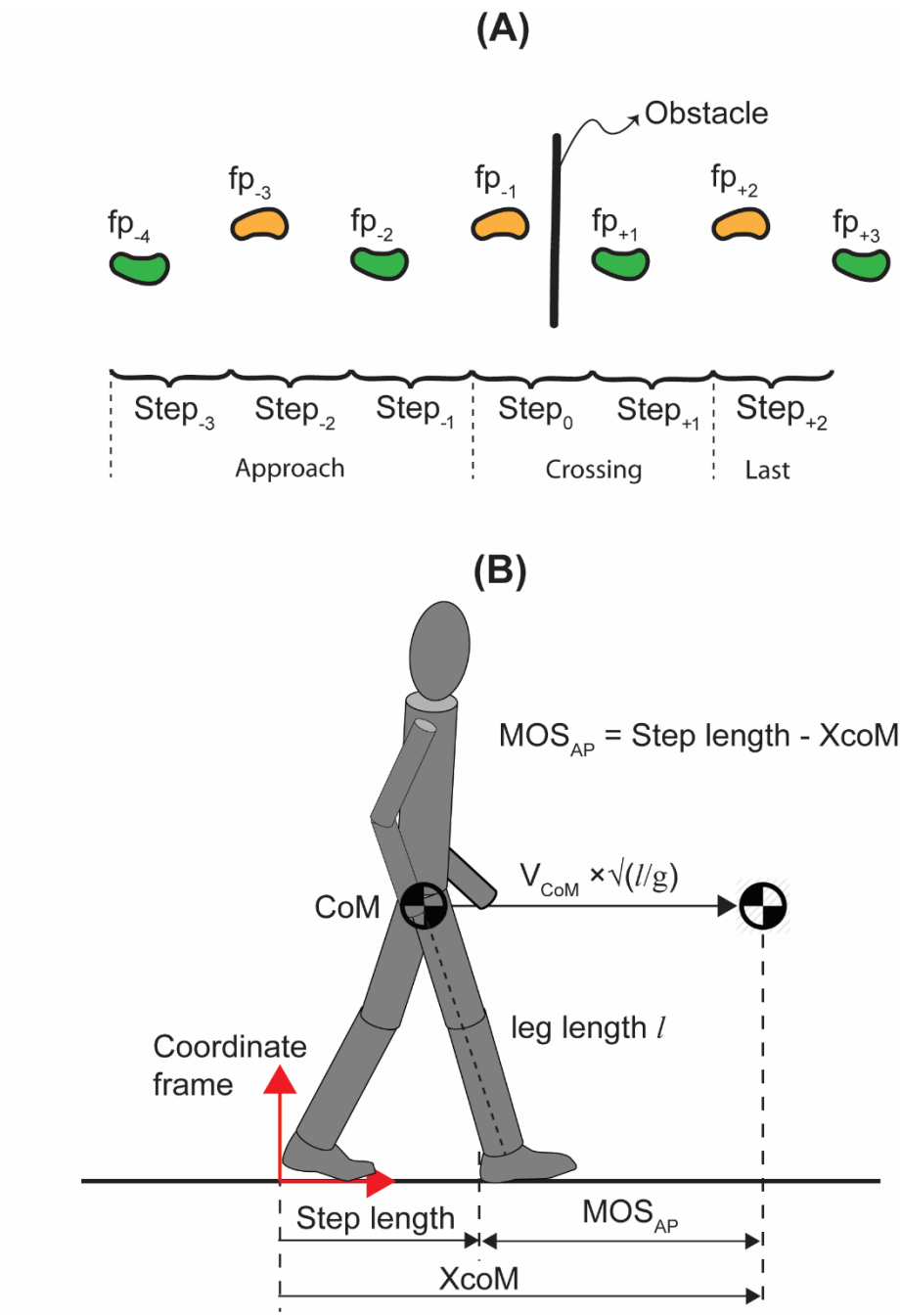

Figure 1. Experimental task and basic definitions. Illustration of foot placements while approaching (fp_{-4} to fp_{-1}), crossing (fp_{+1} and fp_{+2}) and after crossing (fp_{+3}) the obstacle, and of steps while approaching ($Step_{-3}$ to $Step_{-1}$), crossing ($Step_0$ and $Step_{+1}$) and after crossing ($Step_{+2}$) the obstacle **(A)**. Definitions of the extrapolated center of mass (XcoM) and margin of stability, MOS_{AP}. Step length, XcoM and MOS_{AP} are computed at the moment of lead heel contact in a coordinate frame located where the rear heel contacted the ground **(B)**.

2.3 Analysis

Some trials were discarded due to poor kinematic tracking. To have the same number of trials for all participants and tasks, we selected 15 trials with good kinematic data. Fifteen trials are sufficient for reliable quantification of the synergy variables (Rosenblatt and Hurt, 2019). We filtered all kinematic data using a zero-lag, 4th order, low-pass Butterworth filter with a cut-off of 7 Hz. We identified seven foot placements (Fig. 1A) using the AP position of the heel (Desailly et al., 2009). We quantified spatiotemporal gait parameters and margin of stability at heel contact at the seven foot placements (fp_{-4} to fp_{+3}) and six steps ($Step_{-3}$ to $Step_{+2}$; Fig. 1A). Step length was defined as the distance between two consecutive heel contacts. CoM position was computed as the centroid of the triangle formed by the left and right anterior superior iliac spines and the center of the left and right posterior superior iliac spines (Whittle, 1997). CoM velocity was obtained by differentiating the CoM position data. The extrapolated center of mass (XcoM) was calculated in the sagittal plane as (Hof et al., 2005):

$$XcoM = CoM + \frac{V_{CoM}}{\sqrt{\frac{g}{l}}},$$

where CoM is the anterior-posterior CoM position, V_{CoM} is the anterior-posterior CoM velocity, g is the acceleration due to gravity, and l is the participant's leg length (Fig. 1B). Leg length was calculated as the sagittal-plane distance between the CoM and the ankle of the limb that contacted the ground. We used the average of the leg length values obtained from the 15 trials for each step (McAndrew Young et al., 2012). We computed MOS_{AP} at the instant of leading heel contact in a coordinate frame fixed at the location of the rear heel contact (Fig. 1B):

$$MOS_{AP} = Step\ length - XcoM, \qquad (Eqn. 1)$$

i.e., the distance from the anterior boundary of the base of support (BOS), defined by the position of the leading heel, to the XcoM. Negative MOS_{AP} (XcoM ahead of the anterior boundary of the BOS) indicates that the body possesses sufficient momentum to passively rotate over the upright position and fall forward. This is interpreted as instantaneous passive instability in the gait. In contrast, positive MOS_{AP} values (XcoM is behind the anterior boundary of the BOS) indicate that the body does not possess sufficient momentum to rotate beyond the

upright position, and it will eventually fall backward. This is interpreted as instantaneous passive stability, presumably because the rear leg can arrest a backward fall.

We used the uncontrolled manifold (UCM) analysis to quantify the synergy stabilizing MOS_{AP} at heel contact. A *synergy* is co-variation in a redundant sets of input body variables that maintains important output variables that define task performance. The UCM method has been widely used to quantify the synergistic covariation in body variables in a variety of human movements including gait ((Cui et al., 2020, Kulkarni et al., 2021); see (Vaz et al., 2019, Latash and Huang, 2015) for recent reviews). Importantly, while identifying task-specific covariation, the UCM method simultaneously identifies the salient task variables controlled by the nervous system.

Here, we use the UCM method to evaluate the hypothesis that the input variables – step length and XcoM, co-vary to stabilize the output variable, i.e., MOS_{AP}. We performed the analysis separately for each step for both tasks. We first obtain from the constraint equation (Eqn. 1), the Jacobian matrix that relates small changes in the step length and XcoM to changes in MOS_{AP}: $J = [1 \quad -1]$. The one-dimensional null space of this Jacobian defines the UCM, and its one-dimensional compliment defines the orthogonal (ORT) manifold. We pool the across-trial step length and XcoM data for a particular step. The deviation in the step length and XcoM data for each trial from the across-trial mean is projected onto the UCM and the ORT manifolds. The variances in these projections are the V_{UCM} and the V_{ORT}, respectively. These variance components yield the synergy index:

$$\Delta V = \frac{V_{UCM} - V_{ORT}}{\left(\frac{V_{UCM} + V_{ORT}}{2}\right)}.$$

The synergy index ΔV has a threshold value of zero. When $\Delta V > 0$, $V_{UCM} > V_{ORT}$. In general, this implies that the control is organized so that most of the variability in the inputs is channeled along the UCM, and therefore, it does not alter task performance, i.e., the output. Here, $\Delta V > 0$ implies that the step length and XcoM covary to stabilize MOS_{AP}, and we conclude that MOS_{AP} is a controlled variable. Conversely, when $\Delta V < 0$, $V_{UCM} < V_{ORT}$. This implies that most of the variability in the inputs alters task performance. Finally, $\Delta V = 0$ indicates that there is no task-

specific co-variation in the step length and XcoM. Here, $\Delta V \leq 0$ indicates that MOS_{AP} is not a controlled variable.

The synergy index ΔV ranges from -2 to 2. Therefore, it was z-transformed for statistical analysis (Kulkarni et al., 2021, Ambike et al., 2021):

$$\Delta Vz = \frac{1}{2} * \log\left[\frac{2 + \Delta V}{2 - \Delta V}\right].$$

Note that $\Delta V = 0$ translates to $\Delta Vz = 0$. We report ΔVz values in the Results section and use ΔVz values to draw inferences, consistent with most previous studies (Vaz et al., 2019).

2.4 Statistical analysis

To determine whether the synergies were present, we performed separate, one-sample t-tests to test if ΔVz was significantly different from zero for each step in the two tasks (H1). To determine whether the gait task and foot placement affected the synergy index (H2) and MOS_{AP} (H3), we performed a two-way (task × step) repeated measures ANOVA on these variables. To identify the source of changes in the synergy index and in MOS_{AP}, we performed the same ANOVA separately on the variance components (V_{UCM}, V_{ORT}), and on the CoM position, CoM velocity at heel contact and step length, respectively. For all ANOVA tests, we fit a generalized linear model with nested random effects. For the ANOVA on UCM variables and step length, the participant was the random effect. For all other variables, the trial number within each participant was the random effect. Tukey-Kramer adjustments were used to perform the following planned pairwise comparisons: (1) across-task comparison at each of the six steps (or seven foot placements), and (2) all across-step (or foot placement) comparisons for the obstacle-crossing task only. All analyses were performed using the PROC GLIMMIX procedure in SAS 9.4 (Cary, NC, USA) with significance set at 0.05.

3. Results

Figure 2 shows data from one participant and represents the overall results. The figure illustrates (1) the changes in various outcome variables while approaching, crossing, and

resuming gait after crossing an obstacle, and (2) how the variables compare with unobstructed gait for each step. All outcome variables showed a task × step interaction (supporting H2 and H3) indicating that the pattern of changes in the variables across steps was different for the obstacle-crossing task compared to the no obstacle task. The largest across-task changes were observed in all outcomes for the two crossing steps ($Step_0$ and $Step_{+1}$), and across-task changes were apparent in some outcomes in the approach to the obstacle ($Step_{-3}$ to $Step_{-1}$). All variables showed across-step changes for the obstacle-crossing task. The synergy index was greater than zero, indicating that the step length and the XcoM co-varied to stabilize MOS_{AP} for all steps in both tasks (supporting H1). In the detailed results below, we first present the results for the UCM outcome variables describing the stability of MOS_{AP}. Then we present the results for MOS_{AP}, followed by results for the variables that constitute MOS_{AP}: CoM position relative to front heel, CoM velocity at heel contact, and step length.

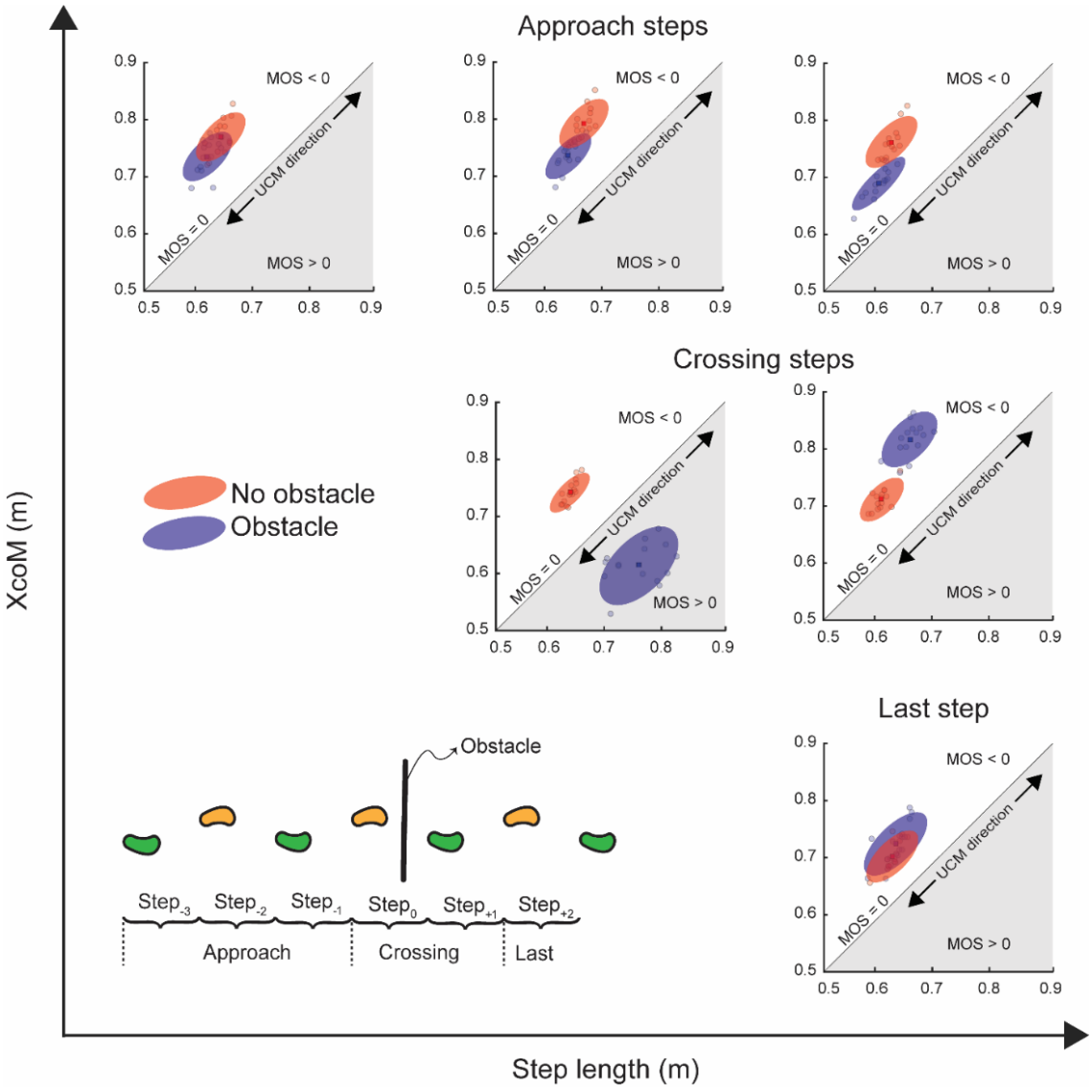

Figure 2. Representative data from one participant. Figure illustrates changes in various outcomes while approaching and crossing an obstacle, and then resuming unobstructed gait (blue ellipses). Steps during unobstructed gait are included for comparison (red ellipses). The 45° line separates the regions of positive and negative MOS_{AP}; the white region above the line represents passively unstable behavior, and the gray region below the line represents passively stable behavior. The 45° line also represents the direction of the uncontrolled manifold (UCM). Variations in step length and XcoM along this direction do not change MOS_{AP}. The ellipses are centered at the centroid of the across-trial data for each step, and the major axes are aligned with the 45° line. However, the flatness of the ellipses is representative. Changes in mean values of the MOS_{AP} are reflected in the position of the ellipses in each chart. The flatness of the ellipse reflects the synergy index, with flatter ellipses indicating higher synergy indices that reflect stronger covariation between the step length and XcoM.

3.1 UCM variables

Synergy index

The synergy index (ΔVz) was significantly greater than zero at all steps for both tasks ($t_{19} < 15.97$, $p < 0.01$; Fig. 3A).

There was a task × step interaction for the synergy index ΔVz ($F_{5,209} = 2.89$, $p = 0.015$; $\eta_p^2 = 0.3$; Fig. 3A). Post-hoc comparisons across tasks revealed that ΔVz was lower during the obstacle-crossing task compared to the no obstacle task for the lead ($step_0$) and trail crossing steps ($step_{+1}$). Post-hoc comparisons across steps for the obstacle-crossing task revealed that ΔVz was lower at the lead crossing step ($step_0$) compared to all non-crossing steps except $step_{-2}$, and ΔVz was lower at the trail crossing step ($step_{+1}$) compared to the last step ($step_{+2}$).

Variance components

There was a task × step interaction for V_{UCM} ($F_{5,209} = 3.12$, $p = 0.009$; $\eta_p^2 = 0.3$; Fig. 3B). Post-hoc comparisons across tasks revealed that V_{UCM} was higher for the obstacle-crossing task compared to the no obstacle task at all but the first two steps ($step_{-3}$ and $step_{-2}$). Post-hoc comparisons across steps for the obstacle-crossing task revealed that V_{UCM} was higher at the lead crossing step ($step_0$) compared to the first two steps ($step_{-3}$ and $step_{-2}$).

There was a task × step interaction for V_{ORT} ($F_{5,209} = 16.51$, $p < 0.001$; $\eta_p^2 = 0.3$; Fig. 3C). Post-hoc comparisons across task revealed that V_{ORT} was higher during the obstacle-crossing task compared to the no obstacle task at the lead ($step_0$) and trail ($step_{+1}$) crossing steps. Post-hoc comparisons across steps for the obstacle-crossing task revealed that V_{ORT} was higher at the lead crossing step ($step_0$) compared to all other steps, and V_{ORT} was higher at the trail crossing step ($step_{+1}$) compared to all steps except the lead crossing step (lower for $step_{+1}$ compared to $step_0$) and the preceding step ($step_{-1}$; no significant difference).

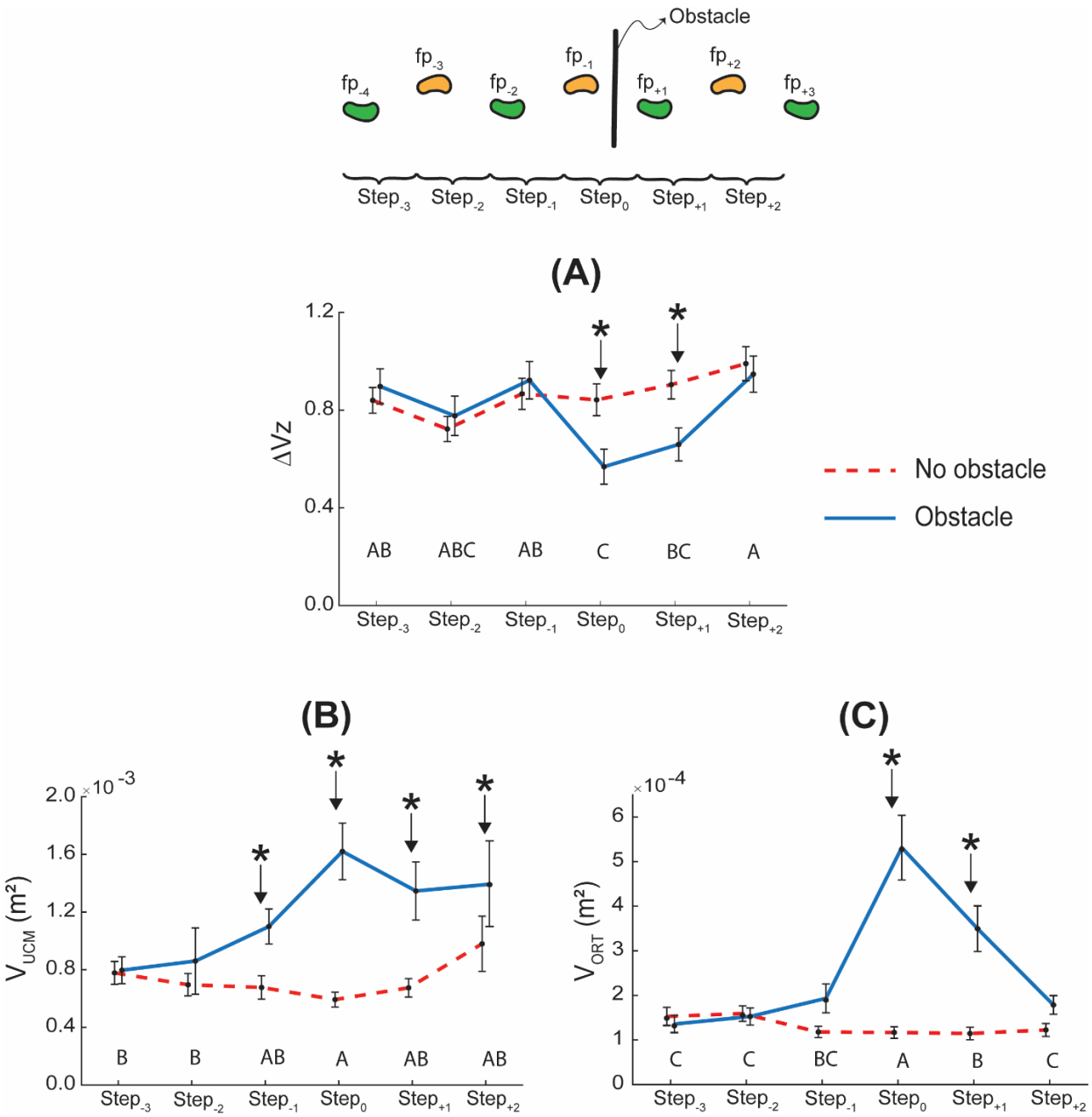

Figure 3. Outcomes of the synergy analysis. Synergy index **(A)**, V_{UCM} **(B)**, and V_{ORT} **(C)**. Data are across-subject means (N=20), and error bars denote standard error. Asterisks denote significant across-task differences at that step ($p < 0.05$). Across-step pairwise comparisons for the obstacle-crossing task are indicated by the row of letters above the horizontal axis for each panel. Steps that do not have letters in common are significantly different from each other (i.e., A is different from B, but A is not different from AB).

3.2 Margin of stability

<u>MOS_{AP}</u>

We observed a task × step interaction for MOS_{AP} ($F_{6,4167} = 886.89$, $p < 0.001$; $\eta_p^2 = 0.9$; Fig. 4A). Post-hoc comparisons across tasks revealed that MOS_{AP} was higher (lower instability) for the obstacle-crossing task than the no obstacle task at all except the first (fp_{-4}) and last two foot placements (fp_{+2} and fp_{+3}). MOS_{AP} was more negative (greater instability) for fp_{+2} (after trail foot crossing) for the obstacle-crossing task. All pair-wise across-step comparisons for the obstacle-crossing task are depicted in Fig. 4A. For brevity, we describe only some of the significant differences. Changes in MOS_{AP} occurred before the obstacle was reached; MOS_{AP} was higher (lower instability) for fp_{-1} relative to the two preceding foot placements. For the two crossing steps, MOS_{AP} first changed from negative to positive for fp_{+1}, and then changed to the most negative value for fp_{+2} relative to all foot placements.

<u>CoM position relative to the rear heel</u>

A task × step interaction was observed for the CoM position relative to the rear heel ($F_{6,4167} = 391.20$, $p < 0.001$; $\eta_p^2 = 0.9$; Fig. 4B). Post-hoc comparisons across tasks revealed that CoM was closer to the rear heel at the foot placements of all approach steps and the lead crossing step (fp_{-4} to fp_{+1}) for the obstacle-crossing task than the no obstacle task. Conversely, CoM was closer to the front heel at the foot placement for the trail crossing step (fp_{+2}) for the obstacle-crossing task. All pair-wise across-step comparisons for the obstacle-crossing task are depicted in Fig. 4B. For brevity, we describe only some of the significant differences. CoM position changed for the last three foot placements. The CoM was closer to the rear foot at the foot placement for the lead crossing step (fp_{+1}). It shifted forward, so that it was closer to the front heel at the foot placement for the trail crossing step (fp_{+2}). Finally, for the last step (fp_{+3}), CoM position was consistent with that for the approach steps.

<u>CoM velocity at heel contact</u>

We observed a task × step interaction for the CoM velocity at heel contact ($F_{6,4167}$= 161.52, $p < 0.001$; $\eta_p^2 = 0.8$; Fig. 4C). Post-hoc comparisons across tasks revealed that the CoM

velocity was lower for the obstacle-crossing task compared to the no obstacle task at all but the first and the last foot placements (fp_{-4} and fp_{+3}). Post-hoc comparisons across steps for the obstacle-crossing task revealed that the CoM velocity was lower at the first (fp_{-4}) and last (fp_{+3}) foot placement compared to other foot placements, except at the lead foot crossing (fp_{+1}), where the CoM velocity was lower compared to all other foot placements.

Step length

We observed a task × step interaction for the step length ($F_{5,3569} = 149.09$; $p < 0.001$; $\eta_p^2 = 0.9$; Fig. 4D). Post-hoc comparisons across tasks revealed that step length was longer during the obstacle-crossing task compared to the no obstacle task at the lead ($step_0$) and trail crossing ($step_{+1}$) steps. Post-hoc comparisons across steps for the obstacle-crossing task revealed that step length increased one step before the crossing step ($step_{-1}$) compared to the first step ($step_{-3}$). Step length was highest for the lead crossing step ($step_0$), and then it shortened for the trail crossing step ($step_{+1}$), but remained longer than all steps except $step_0$. Finally, step length was the shortest for the last step ($step_{+2}$) compared to all other steps.

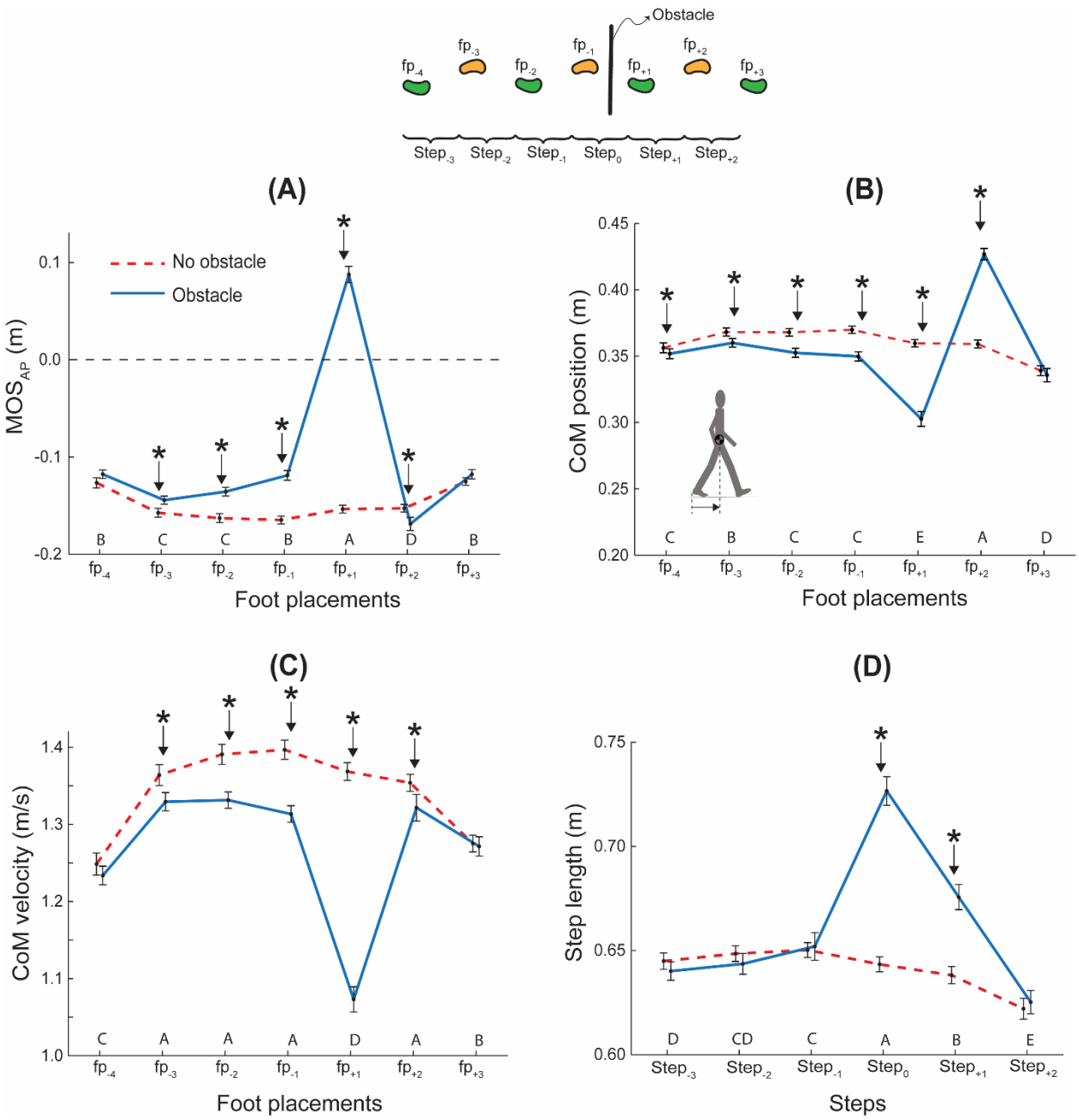

Figure 4. MOS_{AP} and its components. MOS_{AP} **(A)**, CoM position at heel contact **(B)**, CoM velocity at heel contact **(C)** and step length **(D)**. Data are across-subject means (N=20), and error bars denote standard error. Asterisks denote significant task difference at that step ($p < 0.05$). Across-step pairwise comparisons for the obstacle-crossing task are indicated by the row of letters above the horizontal axis for each panel. Steps that do not have letters in common are significantly different from each other (i.e., A is different from B, but A is not different from AB).

4. Discussion

Our goals were to establish that MOS_{AP} is actively controlled during unobstructed as well as obstructed walking, and to quantify any proactive adaptations in MOS_{AP} during obstacle crossing. We report the novel finding that the central nervous system responds to changes in the body's motion with a corresponding correction in step length so that the MOS_{AP} itself is invariant at each heel contact (supporting H1). We also observed that the synergy index was lower while crossing an obstacle compared to earlier and later steps and compared to the corresponding steps during unobstructed gait (supporting H2). Finally, we observed proactive changes in MOS_{AP} in anticipation of a threat to balance; MOS_{AP} changed across steps for unobstructed versus obstructed gait (supporting H3). We argue below that (1) the positive synergy indices indicate that the passive instability is not a byproduct of another process, but that the step length is actively controlled to exploit the unstable passive dynamics to achieve forward progression at low energetic cost; and (2) the proactive changes in the mean MOS_{AP} for the obstacle-crossing task reflect a stability-efficiency tradeoff. Because the MOS_{AP} quantifies the passive dynamic stability of gait, our results indicate that humans employ a *passive dynamics manipulation strategy* to exploit the passive AP body motion to meet specific ends dictated by the locomotor task.

4.1 Active control of MOS_{AP} during unobstructed and obstructed gait

<u>The synergy index provides evidence for the control of MOS_{AP}</u>

The first major finding of this study is that MOS_{AP} is a controlled variable for obstructed as well as unobstructed gait ($\Delta Vz > 0$ for all steps; Fig. 3A). In particular, the synergy index remains significantly larger than zero, even though the input variables that define the MOS_{AP} change over multiple steps for the obstacle-crossing task (Figs 2 and 4), and even when the gait is passively unstable ($MOS_{AP} < 0$ for all but one step in our data). Thus, the UCM analysis provides strong quantitative evidence that MOS_{AP} is controlled.

The variance components (Figs 3B, 3C) provide information regarding the underlying processes that stabilize MOS_{AP}. Higher V_{ORT} indicates higher variability in MOS_{AP}, whereas higher V_{UCM} indicates greater compensatory covariance between XcoM and step length. We

observed that MOS_{AP} is more variable for the crossing steps (up to 205% increase in V_{ORT} compared to earlier steps; Fig. 3C). This likely arises from the larger muscle activations and joint moments required for the crossing steps compared to unobstructed steps (Chou and Draganich, 1997, Haefeli et al., 2011). Higher activations would increase signal-dependent noise (Harris and Wolpert, 1998), which will lead to more variable MOS_{AP}. However, this increase is offset by an increase in V_{UCM} (up to 103% increase compared to earlier steps; Fig. 3B). This compensation leads to MOS_{AP} stabilization overall (Fig. 3A).

<u>Does the synergy arise from passive mechanics, or do neural mechanisms indicate active control?</u>

It is unlikely that passive mechanics of the gait cycle alone can explain the positive synergy indices that we observed. It is indeed likely that mechanics contribute; for example, a greater push off force would result in a more anterior XcoM at the next heel contact, but it would also tend to produce longer steps (Kuo and Donelan, 2010), thereby helping to maintain MOS_{AP}. However, the step length is not entirely determined by a passively swinging leg. Rather, activity in the leg muscles and power at the hip and knee joints indicate active control of the forward swinging limb, which will alter the step length from what a passively swinging limb would yield (Winter, 1991). It is plausible that variations in muscle lengths from their reference values, arising from variations in push off forces, will engage spinal stretch reflexes that will alter step length and contribute to the observed MOS_{AP} synergy (Latash, 2021). This explanation is consistent with the view that for steady state, level gait, humans rely on spinal feedback for control in the AP direction (Bauby and Kuo, 2000, Collins and Kuo, 2013).

The contribution of neural mechanisms to the MOS_{AP} synergy may be even greater for obstructed gait. We observed large fluctuations in the MOS_{AP} over the approach and crossing steps (174% increase for fp_{+1} over fp_{-1}, and a 292% decline for fp_{+2} over fp_{+1}; Fig. 4A). Nevertheless, the synergy index, although lower (38% decline for $Step_0$ relative $Step_{-1}$; Fig. 3A), remained positive. The positive synergy index despite large fluctuations in related variables over consecutive steps suggests the involvement of supraspinal mechanisms. Indeed, supraspinal centers are involved in the control of the obstacle crossing steps (Haefeli et al.,

2011). Spinal reflex responses in the stance leg flexors are enhanced, likely due to increased activity in the prefrontal cortex, in preparation for swinging the leg over the obstacle. Furthermore, the prefrontal cortical activity remains enhanced (compared to unobstructed walking) while swinging the leg over the obstacle (Haefeli et al., 2011). It is also known that visual information about the obstacle is gathered during approach and used to alter gait characteristics (Patla and Vickers, 1997, Diaz et al., 2018). Gathering and using visual information also implicates higher brain centers in the control of obstructed gait, supporting our view that the MOS_{AP} synergy arises from spinal and supraspinal neural circuits. We note both spinal and supraspinal structures are frequently mentioned as candidate neurophysiological bases of synergies (Tillman and Ambike, 2018), although the specific mechanisms are unknown.

Our ideas parallel a similar proposal by Dingwell and colleagues. They investigated step-to-step changes in the MOS in the medio-lateral (ML) direction in externally destabilized environments and argued that MOS_{ML} is controlled during level walking (McAndrew Young et al., 2012, McAndrew Young and Dingwell, 2012, Kazanski et al., 2021). The focus of previous research on ML stability – versus AP stability – is consistent with the view that level gait requires more control along the ML direction, and minimal control along the AP direction (Bauby and Kuo, 2000). The UCM analyses performed here show that the MOS is also controlled in the AP direction by regulating step length – not only in gait tasks that require proactive adaptations, but also during unobstructed gait.

4.2 Proactive changes in MOS_{AP} and the compromise between stability and energy efficiency

The second major finding of this study is that the MOS_{AP} changes while approaching the obstacle. When compared to unobstructed gait, lower instability was apparent three steps before the obstacle (Fig. 4A). Changes in MOS_{AP} during approach and crossing resulted from reduced speed, a more posterior CoM, and increased step length for some steps (Figs. 4B, 4C, 4D). Previous work has demonstrated that changes in MOS_{AP} and MOS_{ML} were evident during the swing phase immediately prior to taking unnaturally long or quick steps (Sivakumaran et al., 2018), and in MOS_{ML} one step before reaching the obstacle (Worden and Vallis, 2016). Here we

extend this finding and demonstrate that MOS_{AP} changes several steps before reaching the obstacle, indicating that the transition from unobstructed to obstructed gait occurs over several steps.

Our findings extend the argument that passive dynamic stability is modulated in response to perceived risk (Hak et al., 2013, Bosse et al., 2012). For example, the substantive increase in MOS_{AP} for the lead crossing step (Figs. 2, 4A) may be a preemptive strategy against a potential trip that will lead to a forward fall (Peebles et al., 2016). Similarly, the even-more-substantive transition back to the most unstable passive dynamics (lowest MOS_{AP}; Fig. 4A) following the trail crossing step may reflect the reduced risk of a forward fall after the trail foot has crossed the obstacle, and the exploitation of passive dynamics to propel the body forward to regain gait speed.

These fluctuations in passive dynamic stability increase the energetic cost of locomotion. The increase in MOS_{AP} over approach steps, and especially the positive MOS_{AP} for the crossing step, indicates that the trailing leg must push off more so that the body can rotate about and beyond the stance ankle. Furthermore, the lead crossing step ($step_0$) is a slower and *longer* step (Figs 3C, 3D), which is inconsistent with the typical combination of a slower and *shorter* step during unobstructed gait which reduces energetic cost (Kuo, 2001, Kuo et al., 2005). Therefore, our results reflect a tradeoff between stability and energy efficiency, consistent with similar arguments offered in the context of stair descent (Bosse et al., 2012), and model-based optimization computations of obstacle crossing behaviors (Chou et al., 1997).

In sum, inspecting changes in MOS_{AP} across tasks and steps leads to the conclusion that MOS_{AP} is proactively adjusted (1) during the approach, likely to facilitate the transition from unobstructed gait to the movements required to clear the obstacle, (2) while crossing an obstacle, likely to prioritize safety over energy optimality, and (3) when resuming level gait to regain gait speed. The large fluctuations in MOS_{AP} reflect a tradeoff between stability and energy efficiency.

4.3 Limitations

We estimated the CoM location using four pelvis markers (Whittle, 1997). A rigorous whole-body model could have provided slightly different estimates of the CoM motion. However, these differences would influence MOS_{AP} similarly across all conditions, and using a different method to obtain CoM kinematics would likely yield similar qualitative results and overall conclusions, especially given the large effect sizes for all our outcome variables. We also observed effects of gait initiation and termination in our data. Gait was initiated one step before the examined steps, and gait was terminated one or two steps after the trail crossing step. Using a longer walkway – with more steps before and after the obstacle – may alter the values of our outcome variables. We do not expect that these changes will influence our key conclusions (control of and proactive changes in MOS_{AP}). However, effects of gait initiation and termination on MOS_{AP} behavior may be worth an independent investigation.

5. Conclusion

We demonstrated that the XcoM and the step length covary to maintain MOS_{AP}, indicating that MOS_{AP} is controlled during unobstructed and obstructed gait. In conjunction with the consistently negative MOS_{AP} values for most of the analyzed steps, we conclude that the MOS_{AP} is controlled to exploit the passive dynamics and achieve forward progression at low energetic cost. Furthermore, the value of MOS_{AP} is proactively altered while approaching an obstacle, and MOS_{AP} shows substantial fluctuations for the two crossing steps. These changes reflect a tradeoff between stability and energy efficiency. The changes during approach and lead crossing steps indicate a growing preference for stability, whereas the opposite change after the trail crossing step indicates a reversion to improving efficiency when the risk to balance is reduced. Thus, our results indicate that humans employ a *passive dynamics manipulation strategy* to exploit the passive AP body motion to meet specific ends dictated by the locomotor task. Given these new insights into AP stability, we conclude that the UCM analysis of MOS_{AP} provides relevant information regarding the control of balance during walking, especially for gait tasks requiring proactive adaptations, and our methods could be valuable in understanding the effects of age and pathology on gait.

Competing Interests

The authors declare no competing or financial interests.

Funding

This work was supported by the Bilsland Dissertation Fellowship awarded by the Office of Interdisciplinary Graduate Programs, and Corrigan Professional Development Grant awarded by the Department of Health and Kinesiology at the university.

Data Availability

All data and code are available at: MOS synergy-Kulkarni et al (2022) All data and code

REFERENCES

AMBIKE, S., PENEDO, T., KULKARNI, A., SANTINELLI, F. B. & BARBIERI, F. A. 2021. Step length synergy while crossing obstacles is weaker in patients with Parkinson's disease. *Gait Posture,* 84**,** 340-345.

BAUBY, C. E. & KUO, A. D. 2000. Active control of lateral balance in human walking. *J Biomech,* 33**,** 1433-40.

BOSSE, I., OBERLANDER, K. D., SAVELBERG, H. H., MEIJER, K., BRUGGEMANN, G. P. & KARAMANIDIS, K. 2012. Dynamic stability control in younger and older adults during stair descent. *Hum Mov Sci,* 31**,** 1560-70.

BRUIJN, S. M., MEIJER, O. G., BEEK, P. J. & VAN DIEEN, J. H. 2013. Assessing the stability of human locomotion: a review of current measures. *J R Soc Interface,* 10**,** 20120999.

CHOU, L. S. & DRAGANICH, L. F. 1997. Stepping over an obstacle increases the motions and moments of the joints of the trailing limb in young adults. *J Biomech,* 30**,** 331-7.

CHOU, L. S., DRAGANICH, L. F. & SONG, S. M. 1997. Minimum energy trajectories of the swing ankle when stepping over obstacles of different heights. *J Biomech,* 30**,** 115-20.

COLLINS, S. H. & KUO, A. D. 2013. Two independent contributions to step variability during over-ground human walking. *PLoS One,* 8**,** e73597.

CUI, C., KULKARNI, A., RIETDYK, S., BARBIERI, F. A. & AMBIKE, S. 2020. Synergies in the ground reaction forces and moments during double support in curb negotiation in young and older adults. *J Biomech,* 106**,** 109837.

DESAILLY, E., DANIEL, Y., SARDAIN, P. & LACOUTURE, P. 2009. Foot contact event detection using kinematic data in cerebral palsy children and normal adults gait. *Gait Posture,* 29**,** 76-80.

DIAZ, G. J., PARADE, M. S., BARTON, S. L. & FAJEN, B. R. 2018. The pickup of visual information about size and location during approach to an obstacle. *PLoS One,* 13**,** e0192044.

HAEFELI, J., VOGELI, S., MICHEL, J. & DIETZ, V. 2011. Preparation and performance of obstacle steps: interaction between brain and spinal neuronal activity. *Eur J Neurosci,* 33**,** 338-48.

HAK, L., HETTINGA, F. J., DUFFY, K. R., JACKSON, J., SANDERCOCK, G. R. H. & TAYLOR, M. J. D. 2019. The concept of margins of stability can be used to better understand a change in obstacle crossing strategy with an increase in age. *J Biomech,* 84**,** 147-152.

HAK, L., HOUDIJK, H., BEEK, P. J. & VAN DIEEN, J. H. 2013. Steps to take to enhance gait stability: the effect of stride frequency, stride length, and walking speed on local dynamic stability and margins of stability. *PLoS One,* 8**,** e82842.

HARRIS, C. M. & WOLPERT, D. M. 1998. Signal-dependent noise determines motor planning. *Nature,* 394**,** 780-4.

HOF, A. L. 2008. The 'extrapolated center of mass' concept suggests a simple control of balance in walking. *Hum Mov Sci,* 27**,** 112-25.

HOF, A. L., GAZENDAM, M. G. & SINKE, W. E. 2005. The condition for dynamic stability. *J Biomech,* 38**,** 1-8.

KAZANSKI, M., CUSUMANO, J. P. & DINGWELL, J. B. 2021. Rethinking Margin of Stability: Incorporating Step-To-Step Regulation to Resolve the Paradox. *bioRxiv*.

KULKARNI, A., CHO, H., RIETDYK, S. & AMBIKE, S. 2021. Step length synergy is weaker in older adults during obstacle crossing. *J Biomech,* 118**,** 110311.

KUO, A. D. 2001. A simple model of bipedal walking predicts the preferred speed-step length relationship. *J Biomech Eng,* 123**,** 264-9.

KUO, A. D. & DONELAN, J. M. 2010. Dynamic principles of gait and their clinical implications. *Phys Ther,* 90**,** 157-74.

KUO, A. D., DONELAN, J. M. & RUINA, A. 2005. Energetic consequences of walking like an inverted pendulum: step-to-step transitions. *Exerc Sport Sci Rev,* 33**,** 88-97.

LATASH, M. L. 2021. One more time about motor (and non-motor) synergies. *Exp Brain Res,* 239**,** 2951-2967.

LATASH, M. L. & HUANG, X. 2015. Neural control of movement stability: Lessons from studies of neurological patients. *Neuroscience,* 301**,** 39-48.

MCANDREW YOUNG, P. M. & DINGWELL, J. B. 2012. Voluntarily changing step length or step width affects dynamic stability of human walking. *Gait Posture,* 35**,** 472-7.

MCANDREW YOUNG, P. M., WILKEN, J. M. & DINGWELL, J. B. 2012. Dynamic margins of stability during human walking in destabilizing environments. *J Biomech,* 45**,** 1053-9.

MUIR, B. C., HADDAD, J. M., VAN EMMERIK, R. E. A. & RIETDYK, S. 2019. Changes in the control of obstacle crossing in middle age become evident as gait task difficulty increases. *Gait Posture,* 70**,** 254-259.

OHTSU, H., YOSHIDA, S., MINAMISAWA, T., KATAGIRI, N., YAMAGUCHI, T., TAKAHASHI, T., YOMOGIDA, S. I. & KANZAKI, H. 2020. Does the balance strategy during walking in elderly persons show an association with fall risk assessment? *J Biomech,* 103**,** 109657.

OHTSU, H., YOSHIDA, S., MINAMISAWA, T., TAKAHASHI, T., YOMOGIDA, S. I. & KANZAKI, H. 2019. Investigation of balance strategy over gait cycle based on margin of stability. *J Biomech,* 95**,** 109319.

PATLA, A. E. & VICKERS, J. N. 1997. Where and when do we look as we approach and step over an obstacle in the travel path? *Neuroreport,* 8**,** 3661-5.

PEEBLES, A. T., REINHOLDT, A., BRUETSCH, A. P., LYNCH, S. G. & HUISINGA, J. M. 2016. Dynamic margin of stability during gait is altered in persons with multiple sclerosis. *J Biomech,* 49**,** 3949-3955.

RAFFEGEAU, T. E., BRINKERHOFF, S. A., KELLAHER, G. K., BAUDENDISTEL, S., TERZA, M. J., ROPER, J. A. & HASS, C. J. 2022. Changes to margins of stability from walking to obstacle crossing in older adults while walking fast and with a dual-task. *Exp Gerontol,* 161**,** 111710.

ROSENBLATT, N. J. & HURT, C. P. 2019. Recommendation for the minimum number of steps to analyze when performing the uncontrolled manifold analysis on walking data. *Journal of biomechanics,* 85**,** 218-223.

SCHOLZ, J. P. & SCHONER, G. 1999. The uncontrolled manifold concept: identifying control variables for a functional task. *Exp Brain Res,* 126**,** 289-306.

SIVAKUMARAN, S., SCHINKEL-IVY, A., MASANI, K. & MANSFIELD, A. 2018. Relationship between margin of stability and deviations in spatiotemporal gait features in healthy young adults. *Hum Mov Sci,* 57**,** 366-373.

TILLMAN, M. & AMBIKE, S. 2018. Cue-induced changes in the stability of finger force-production tasks revealed by the uncontrolled manifold analysis. *J Neurophysiol,* 119**,** 21-32.

TILLMAN, M. & AMBIKE, S. 2020. The Influence of Recent Actions and Anticipated Actions on the Stability of Finger Forces During a Tracking Task. *Motor Control,* 24**,** 365-382.

VAZ, D. V., PINTO, V. A., JUNIOR, R. R. S., MATTOS, D. J. S. & MITRA, S. 2019. Coordination in adults with neurological impairment - A systematic review of uncontrolled manifold studies. *Gait Posture,* 69**,** 66-78.

WHITTLE, M. W. 1997. Three-dimensional motion of the center of gravity of the body during walking. *Human Movement Science,* 16**,** 347-355.

WINTER, D. A. 1991. *The Bionechanics and Motor Control of Human Gait: Normal, Elderly and Pathological,* Kitchener, ON, Waterloo Biomechanics.

WORDEN, T. A. & VALLIS, L. A. 2016. Stability control during the performance of a simultaneous obstacle avoidance and auditory Stroop task. *Exp Brain Res,* 234**,** 387-96.

Figure Captions

Figure 1. Experimental task and basic definitions. Illustration of foot placements while approaching (fp_{-4} to fp_{-1}), crossing (fp_{+1} and fp_{+2}) and after crossing (fp_{+3}) the obstacle, and of steps while approaching ($Step_{-3}$ to $Step_{-1}$), crossing ($Step_0$ and $Step_{+1}$) and after crossing ($Step_{+2}$) the obstacle **(A)**. Definitions of the extrapolated center of mass (XcoM) and margin of stability, MOS_{AP}. Step length, XcoM and MOS_{AP} are computed at the moment of lead heel contact in a coordinate frame located where the rear heel contacted the ground **(B)**.

Figure 2. Data from one representative participant. Figure illustrates changes in various outcomes while approaching and crossing an obstacle, and then resuming unobstructed gait (blue ellipses). Steps during unobstructed gait are included for comparison (red ellipses). The 45° line separates the regions of positive and negative MOS_{AP}; the white region above the line represents passively unstable behavior, and the gray region below the line represents passively stable behavior. The 45° line also represents the direction of the uncontrolled manifold (UCM). Variations in step length and XcoM along this direction do not change MOS_{AP}. The ellipses are centered at the centroid of the across-trial data for each step, and the major axes are aligned with the 45° line. However, the flatness of the ellipses is representative. Changes in mean values of the MOS_{AP} are reflected in the position of the ellipses in each chart. The flatness of the ellipse reflects the synergy index, with flatter ellipses indicating higher synergy indices that reflect stronger covariation between the step length and XcoM.

Figure 3. Outcomes of the synergy analysis. Synergy index **(A)**, V_{UCM} **(B)**, and V_{ORT} **(C)**. Data are across-subject means (N=20), and error bars denote standard error. Asterisks denote significant across-task differences at that step ($p < 0.05$). Across-step pairwise comparisons for the obstacle-crossing task are indicated by the row of letters above the horizontal axis for each panel. Steps that do not have letters in common are significantly different from each other (i.e., A is different from B, but A is not different from AB).

605 **Figure 4. MOS_{AP} and its components.** MOS_{AP} **(A)**, CoM position at heel contact **(B)**, CoM
606 velocity at heel contact **(C)** and step length **(D)**. Data are across-subject means (N=20), and
607 error bars denote standard error. Asterisks denote significant task difference at that step ($p <$
608 0.05). Across-step pairwise comparisons for the obstacle-crossing task are indicated by the row
609 of letters above the horizontal axis for each panel. Steps that do not have letters in common
610 are significantly different from each other (i.e., A is different from B, but A is not different from
611 AB).

612

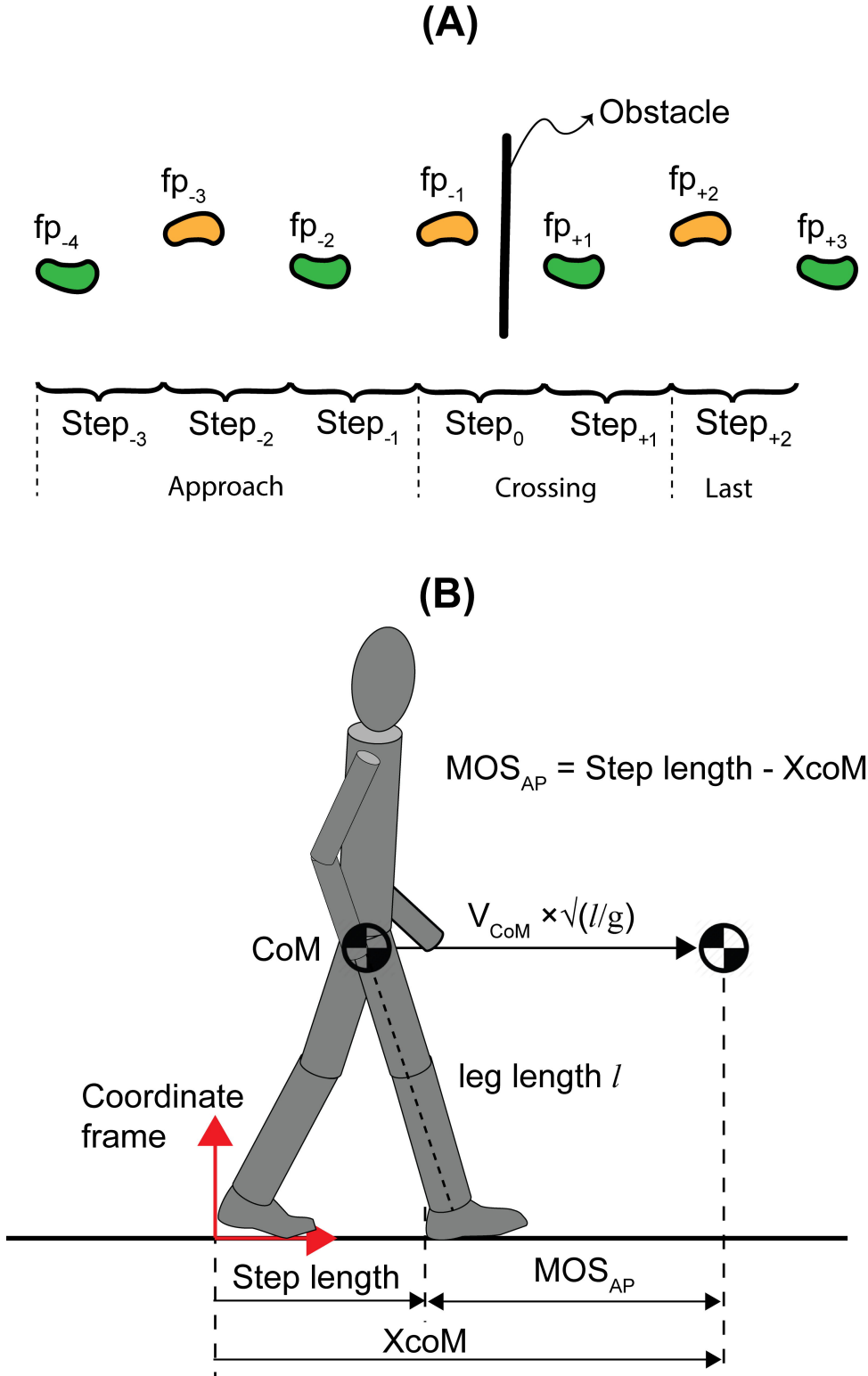
(A)
Obstacle
fp-4
fp-3
fp-2
fp-1
fp+1
fp+2
fp+3
Step-3
Step-2
Step-1
Step0
Step+1
Step+2
Approach
Crossing
Last
(B)
MOSAP = Step length - XcoM
VCoM ×√(l/g)
CoM
leg length l
Coordinate frame
Step length
MOSAP
XcoM

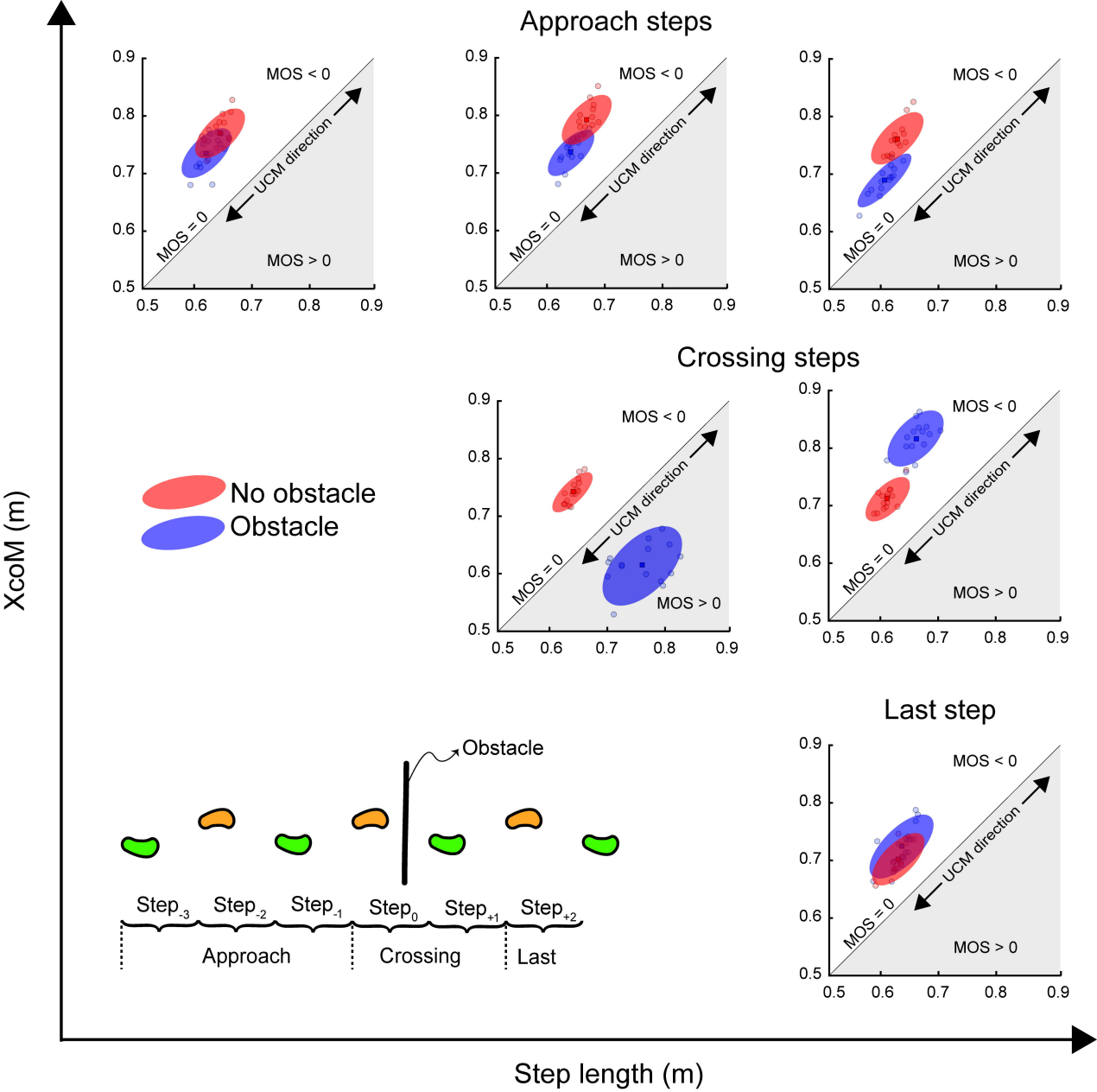
Approach steps
Crossing steps
Last step
MOS < 0
MOS > 0
MOS = 0
UCM direction
0.5
0.6
0.7
0.8
0.9
No obstacle
Obstacle
Obstacle
Step-3
Step-2
Step-1
Step0
Step+1
Step+2
Approach
Crossing
Last
XcoM (m)
Step length (m)

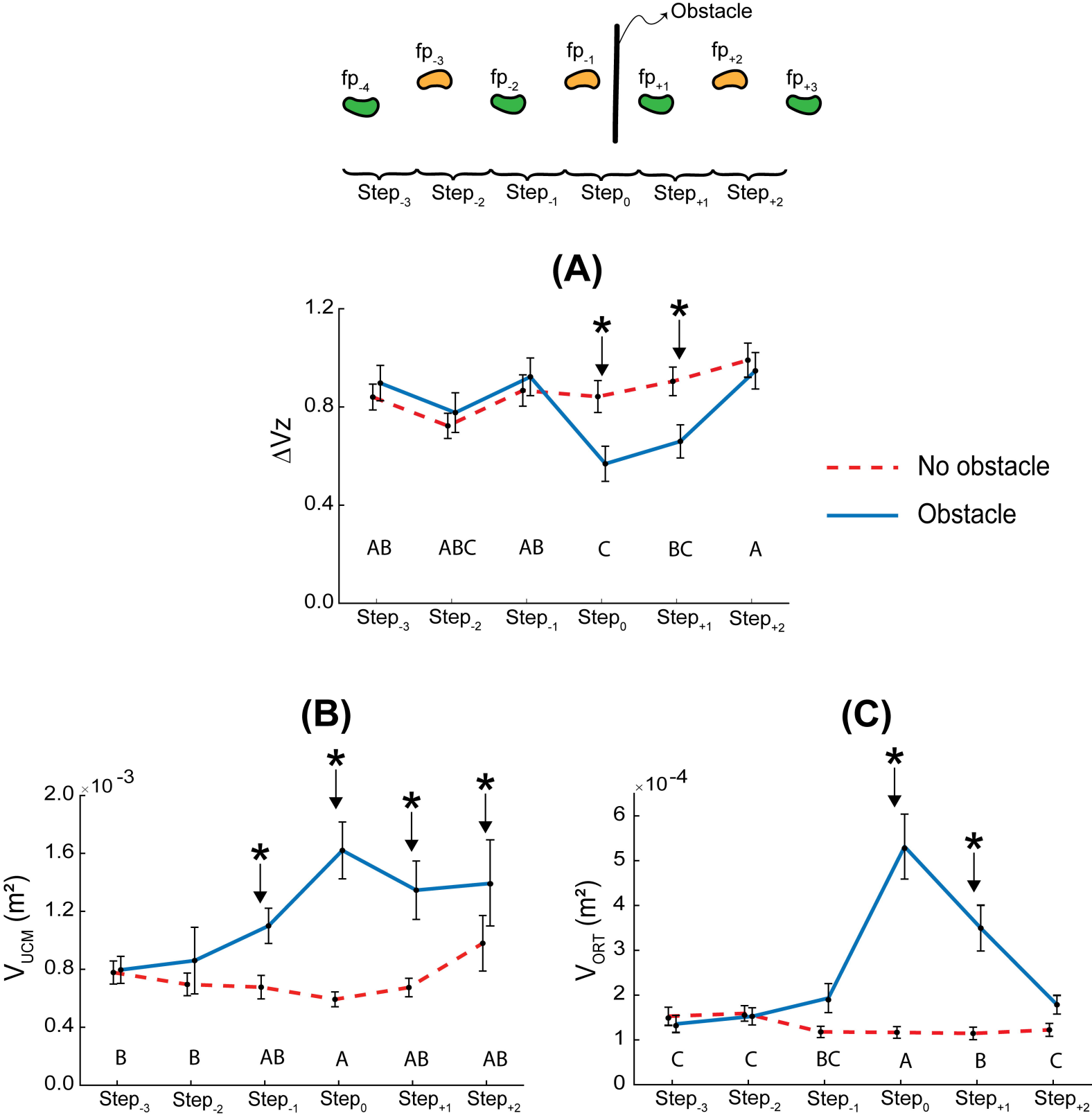
Obstacle
fp-4
fp-3
fp-2
fp-1
fp+1
fp+2
fp+3
Step-3
Step-2
Step-1
Step0
Step+1
Step+2
(A)
ΔVz
1.2
0.8
0.4
0.0
AB
ABC
AB
C
BC
A
No obstacle
Obstacle
(B)
×10-3
2.0
1.6
1.2
0.8
0.4
0.0
VUCM (m2)
B
B
AB
A
AB
AB
(C)
×10-4
6
5
4
3
2
1
0
VORT (m2)
C
C
BC
A
B
C

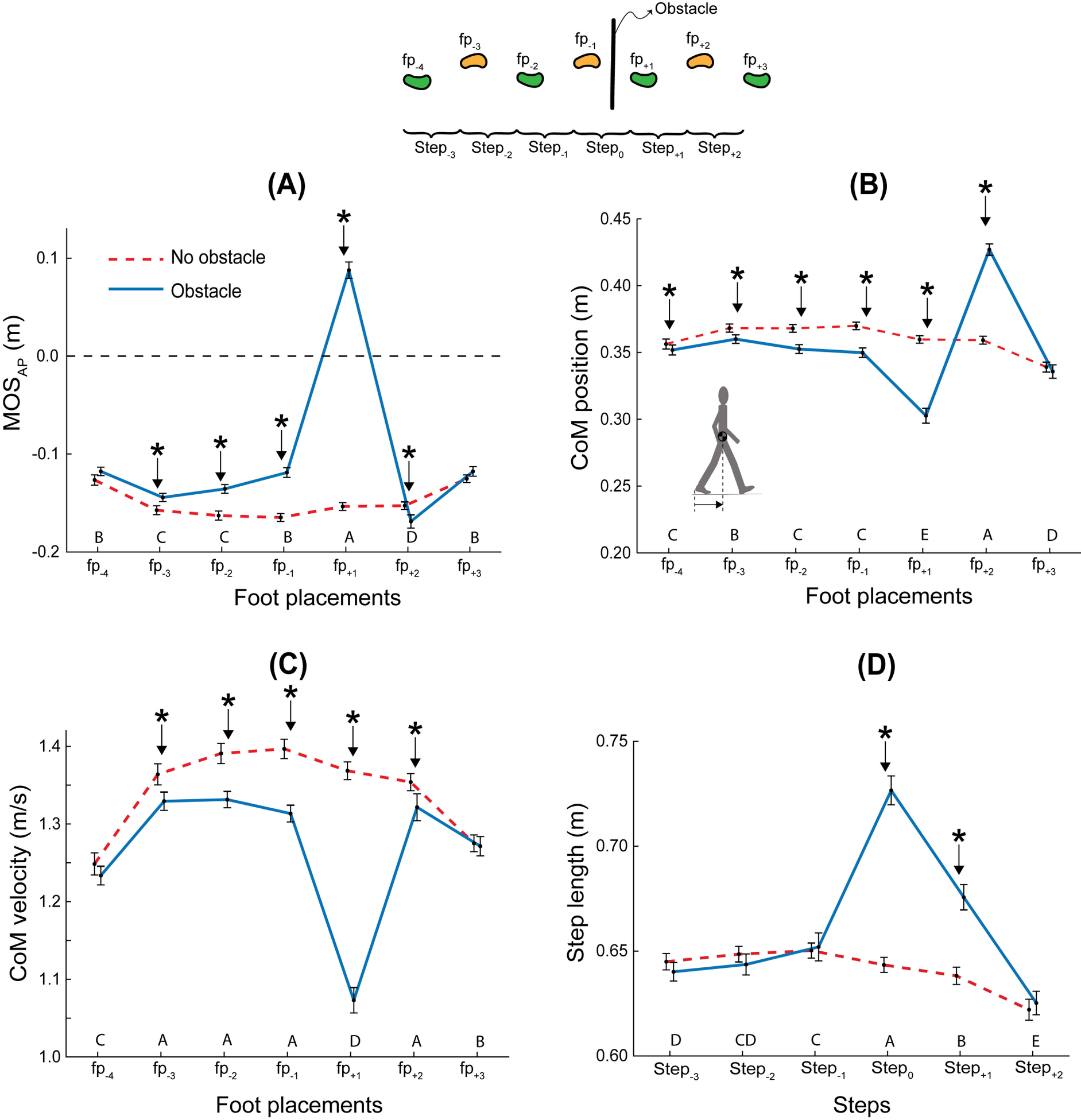
Obstacle
fp-4
fp-3
fp-2
fp-1
fp+1
fp+2
fp+3
Step-3
Step-2
Step-1
Step0
Step+1
Step+2
(A)
No obstacle
Obstacle
MOSAP (m)
0.1
0.0
-0.1
-0.2
B C C B A D B
Foot placements
(B)
CoM position (m)
0.45
0.40
0.35
0.30
0.25
0.20
C B C C E A D
Foot placements
(C)
CoM velocity (m/s)
1.4
1.3
1.2
1.1
1.0
C A A A D A B
Foot placements
(D)
Step length (m)
0.75
0.70
0.65
0.60
D CD C A B E
Steps